On the Influence of Collector Size on the Solar Chimneys Performance

Sundus S. Al-Azawiey[2], *Hussain H.* Al-Kayiem[1,*], and *Suhaimi B* Hassan[1]

[1] *Mechanical Engineering Department, Universiti Teknologi PETRONAS, 32610 Bandar Seri Iskandar, Malaysia*
[2] *Electromechanical Engineering Department, University of Technology, Baghdad, Iraq*

Abstract. Performance of solar chimney power plant system is highly influenced by the design geometries. The collector size is logically enhances the solar chimney performance, but the trend of enhancement is not yet investigated. In the present work, experimental and numerical investigations have been carried out to ascertain, in terms of qualitative and quantitative evaluation, the effect of the collector diameter. Daily thermal efficiency has been determined at four different collector diameter. Two different collector diameters, 3.0 and 6.0 m, have been investigated experimentally, and then scaled up, to 9.0 and 12.0 m, by numerical simulation using ANSYS-FLUENT®15 software. Results demonstrated that collector diameter has effectively influenced the system performance. Larger collector diameter imposed increase in the velocity, temperature and the daily average thermal efficiency of the system. From the experimental results, increasing the collector diameter from 3.0 to 6.0 m has increased the daily average thermal efficiency of the collector from 9.81 to 12.8. Simulation results at 800 W/m^2 irradiation revealed that the velocity in the chimney have increased from 1.66 m/s at 3.0 m collector diameter to 2.34, 2.47 and 2.63 m/s for 6.0, 9.0 and 12.0 m collector diameters, respectively.

1 Introduction

The concept of solar energy induced updraft has been used for ventilation, power generation, drying and space heating. The use of solar updraft for electrical power generation using SCPP was first conceived in 1903 by a Spanish Artillery Colonel, Isadora Cabanyes in his "Proyecto de motor solar" (solar engine project) [1, 2]. In 1926, Prof. Bernard Dubos suggested the use of mountain slope as support to the chimney [3, 4]. SCPP gained attention in 1978 when Prof. Schlaich presented the SCPP technology in a congress [5]. Between 1980 and 1982, Prof Schlaich and his colleagues designed and constructed the first pilot SCPP on a site provided at Manzanares by the Spanish Utility Union Electrica Fenosa with funding from the German Ministry of Research and Technology [6-8].

SCPP collector component is the solar energy conversion component of the SCPP which converts solar energy to thermal energy and subsequently to kinetic energy in the air.

* Corresponding author: hussain_kayiem@utp.edu.my

Thus, the energy conversion process in the collector involves the absorption of solar radiation by the absorber/ground to thermal energy in the absorber, heat transfer from the absorber to adjacent air generating air in motion and the diving of the turbine by the buoyant air to generate electricity. The mass flow rate of the buoyant air at the collector exit/chimney base is a major determinant of the total power output expected from the plant. In his theses, [9] reported that the collector contributes about 50% of the total loss in a SCPP, which are mostly thermal losses to the atmosphere. To reduce the frictional drag, Bonnelle [10] proposed another design of air flow guides to direct the generated buoyant air towards the chimney, thus reduces the air circulation at the collector and reduces heat losses, as well.

Ref. [11] introduced the use of intermediate secondary cover/roof in the collector to reduce the losses. The intermediate roof divides the collector into top and bottom parts where the convective heat loss from the buoyant air generated from the bottom part of the collector is utilized to generate hot air at the top partition of the collector. To reduce air resident time in the collector and consequently reduce the convective loss from the air, [12] proposed a SCPP with inclined solar collector for high latitude location. Their claim is that the system had higher performances for locations at high latitudes than the use of traditional SCPP in same location. This claim might be as a result of increase radiation capturing and reduced frictional losses at the collector section for sloped collector, thus the thermal losses through the cover was reduced. Ref. [13] employed Constructal Design to evaluate analytically the effect the ratio between height of chimney and radius of collector over the power production for a reference plant. In spite of application of the same method for geometrical evaluation, the work brings different findings than [14] results.

It is obvious that most of the reported results and suggestions haven't included the influence of the size of the SAC on the performance of the SC. On the other hand, most of the works have been carried out numerically and mathematically. The literature suffers the lack for experimental data to be utilized for design of the SC, and also for validation of the numerical procedures that may be carried out by other researchers.

The present work intended to presents results on the SC performance under different collector sizes by experimental and numerical analyses. Experimental measurements have been repeated for two different collector diameters, 3.0 and 6.0 m. Numerical simulation has been carried out to extend the investigation to of 9.0 and 12.0 m collector diameter.

2 Experimental methodology

The experimental model of the SC was implemented in the Solar Research Site under the actual environmental condition at the location, Universiti Teknologi PETRONAS – Malaysia (latitude 4.39^{o}N, 100.98^{o}E).

Description of the experimental model

The experimental model of the solar chimney has a collector, chimney and power generation unit. The collector was 3.0 m diameter and then extended to 6.0 m with canopy made from Perspex, while the absorber was made of ground covered by black painted pebble. Water retention on the canopy surface has been considered, and hence it was designed with a slope. The chimney was 6.3 m height made of 152.5 mm (6.0") diameter PVC pipe installed in the center above the collector. The inlet of the canopy height above the ground was 0.05 m, for both 3.0 and 6.0 m collector diameter. The layout of the solar chimney model is shown in Figure1.

The collector thermal efficiency was calculated by equations (1).

DOI: 10.1051/matecconf/201713102011

$$\eta_{coll} = \frac{q_u}{Q_{solar} + Q_{TES}} = \frac{q_u}{I \cdot A_{coll} + Q_{TES}} \tag{1}$$

Where: q_u useful energy gained

Q_{solar} is the energy gained from the solar radiation, which is the product of the global horizontal solar radiation, I, and the collector area, A_{coll}. Q_{TES} is the energy released from the TES to the air, expressed as equations (2)

$$Q_{TES} = m_{TES} \times c_{p.TES} \times (T_{TES,2} - T_{TES,1}) / 3600 \tag{2}$$

Where: $T_{TES.2}$ and $T_{TES.1}$ are the ground temperatures at the end and beginning of the measurement hours.

Measuring Instrumentations and Procedure

The instrumentation of the system was designed to capture all the components as a solar radiation, temperatures and velocities. The data generated from the experiments were used to determine the system performances under the various conditions following the experimental plans.

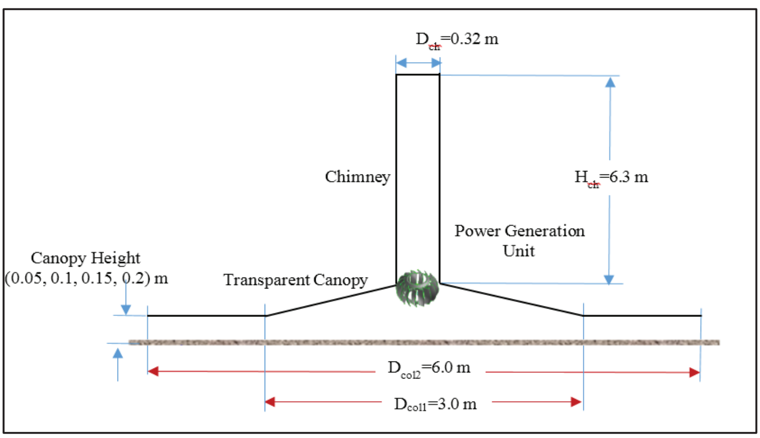

Fig. 1. Outlines of the experimental setup

The thermal performance of the system could only be determined through the measurement of the temperatures of all the components of the system and the temperature changes in the process. To get the temperature data at the different components of the system, the system was instrumented with thirteen thermocouples to collect the temperature data at the absorber surface, transparent cover material, air inside chimney, air in the collector and ambient air. All the thermocouples used for this study were Type J thermocouples, which included probe types used for air temperature and surfaces type for wall temperature measurements. To record the temperature values, all the thermocouples were connected to GRAPHTEC 820 data logger for instant temperature data collection and safe storage the record was every 5 mints and calculated the average of every one hours. For air velocities at the solar chimney model were measured at two different locations in the chimney using portable hotwire probe anemometer. The hotwire probe anemometer has accuracy of ±3% of reading or ±0.03 m/s. The ambient air velocity in the site was measured using portable thermo-anemometer. The global solar radiation was measured at the solar site in UTP using KIMO Solarimeter (SL200) which has measuring accuracy of ±5%.

3 Numerical methodology

The simulation procedure, using CFD technique, to analyze the fluid flow and thermal processes in the solar chimney is described in this section. Since the temperature is essential parameter in the process of solar energy conversion, software package ANSYS-FLUENT®15 was used.

Development of numerical model

Two different models have been created in this simulation. They are duplication of the experimental models. The first model was with 3.0 m diameter and the collector has 15^{o} inclination, as shown in Figure 1. In the second model, the collector diameter was increased to 6.0 m. The extended canopy part has 5^{o} inclination which is sloped towards the peripheral of the collector. The chimney has similar geometries of the experimental model. The ground, functioning as absorber, was simulated as TES made of black painted pebbles.

Mesh generation and mesh independency

The meshing criterion was structured of Tet/Hybrid cells type due to the sharp and curved edges in the flow passages. To study the independency of the results on the mesh, four different mesh sizes, coarse, medium, fine and finer were generated using the second model of 6.0 m diameter. The four different sizes of cells where used to predict the temperatures and air velocities in the chimney base. The mesh checking has been carried out with 0.05 m canopy height when the solar radiation was 800 W/m^2 and ambient temperature 33^{o}C. Predicted temperatures and velocities by mesh with 988.499 cells have close results to the mesh results of 413571 cells with less than 1.0% error in the predicted both temperature and velocity. The results of the mesh with 413571 cells simulation was considered to continue the simulation at various boundary and design conditions. Table 1 shows the details for grid generation and grid Independency for SC model.

Table 1. Grid generation and grid independency for SC model.

Grid type	Grid sizes (No. of cells)	Grid dependent Parameters			
		Velocity at chimney base, $V_{ch.avg}$ (m/s)	Error (%)	Temperature at chimney base, T_{ch} (K)	Error (%)
Coarse Mesh	61165	1.38	38	317.8	2.93
Medium Mesh	195333	1.99	11.1	320.0	2.26
Fine Mesh	413571	2.22	0.89	327.0	0.12
Finer Mesh	988,499	2.24	-	327.4	-

Boundary conditions

For SC model, different boundary conditions were set for the different parts of the system and different materials. The ground material used in the entire simulation was black painted pebbles, collector roof material was Perspex, and the chimney wall material was

DOI: 10.1051/matecconf/201713102011

PVC. The materials were defined in the system with the different thermo-physical properties of the components and the operating fluid, air. The boundary conditions used in the simulation are presented in Table 2.

Table 2. Boundary conditions for the simulation of SC model.

Component	Boundary type	Value
Ground	Wall	Constant heat flux
Collector	Wall	Constant heat flux
Chimney	Wall	Adiabatic, $q = 0$ W/m^2
Collector inlet	Pressure inlet	$P_{inlet} = 0$ Pa, $T_{in} = T_{amb}$

4 Results and discussion

4.1 Experimental results

In this work, the measurements have been acquired over 24 hours daily for four days repeatability. The behavior of the collector with 3.0 and 6.0 m diameter is interesting and never being reported before. From figure 2, which shows the determined thermal efficiency of the collector over 24 hours, there is inconsistent behavior of the system between the day and in the night. During the sun hours, from 8.00AM to 8.00PM, the 3 m collector has efficiency higher than the 6.0 m collector. The reason is the larger area of the collector processes higher thermal losses to the environment, and also as frictional drag to the air flow inside the collector.

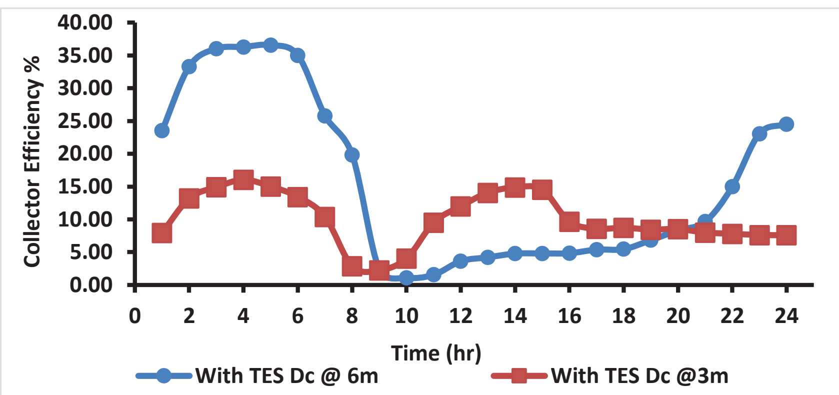

Fig. 2. Measured thermal efficiency at 3.0 and 6.0 m collector diameter over 24 hour (mean of four days repeatability)

In addition, the larger size of the TES absorbs larger amount of solar radiation and store it as heat and start to discharge the stored heat after sunset. Because the amount of stored heat in the case of 6.0 m collector, the heat supplied to the air inside the collector is higher compared to the amount of heat supplied to the air in 3.0 m case. This is why the 6.0 m collector diameter resulted in high collector thermal efficiency in the night.

DOI: 10.1051/matecconf/201713102011

4.2 Numerical results

The collector area effect on the SC performance in this work has been extended from the experimental investigation at 3.0 and 6.0 m to numerical investigation at 9.0 and 12.0 m collector diameter. The obtained results from the simulation have been presented in terms of air velocity, temperature and system thermal efficiency. The simulation considered 800 W/m^2 solar irradiance and prevalent ambient condition at the location when the solar intensity is between 700 W/m^2 and 900 W/m^2, which is at an average temperature of 33°C. The simulation considered optimum canopy height as captured in independent analysis from the experimental investigation.

The results showed that the velocity at optimum canopy height varied with collector diameter, as shown in Figure 3. This is because the air in the greenhouse gains the required thermal energy that can excite the internal energy and induce buoyancy.

By referring back to the experimental results, the measured velocity for the 6.0 m collector diameter is 2.25 m/s. The corresponding numerical result is 2.34. It could be seen that the percentage of error is 4%. This indicates the good agreement between the experimental and numerical analysis.

Figure 4 shows the simulation results of air velocity in vector contours, for 3.0 m collector diameter. Air velocity has a small radial component compared to the vertical component. The vertical component overrides the radial component because the distance from the ground to the canopy is relatively large as compared to the radial passage. The flow moves mostly up and reaches the canopy and return back with reversal manner, towards the chimney base. Once the outer narrow passage flow reaches the central part, it could gain larger vertical velocity component, due to the area enlargement of the configuration, in the vertical direction. However, the resultant of the flow direction was noted to be mainly towards the chimney base, due the stack effect.

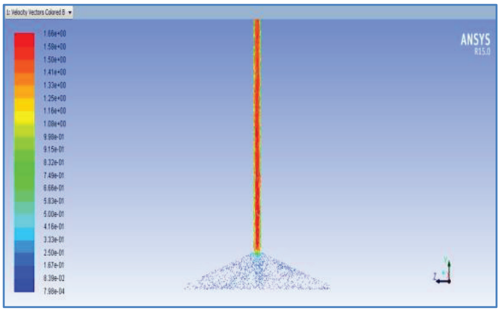

Fig. 4. Air velocity vector at 3.0 m collector diameters; 800 W/m^2 solar irradiance.

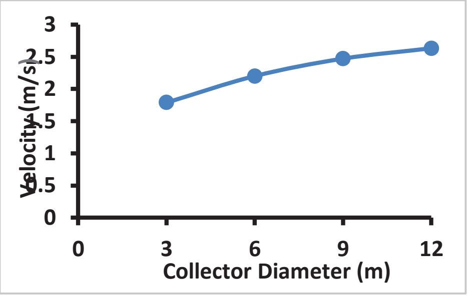

Fig. 3. Air velocity at different collector diameters

4.3 Validation of numerical simulation

Prior to carry forward on the numerical investigations, a level of confident has been established by validation process. The experimental results at 3.0 and 6.0 m collector diameter have been compared with the numerical results under similar conditions of ~800 W/m^2 irradiance and ~33°C ambient temperature.

In terms of velocity at the chimney, the comparison is shown in Table 3. Result of the simulation, in comparison with the experimental results showed small higher predicted velocity values. At 3.0 m collector diameter, the experimentally measured velocity at the chimney base was 1.56 m/s while the predicted one by the simulation was 1.6 m/s with difference of 2.5%. For the 6.0 m collector diameter, the experimental result was 2.25 m/s

 DOI: 10.1051/matecconf/201713102011

and the numerical result was 2.34 m/s, with difference of 2.22%. This margin of error represents acceptable accuracy of the numerical procedure.

Table 3: Comparison of Numerical and Experimental Velocity results for 3.0 m and 6.0 m Collector diameters.

D = 3.0 m				D = 6.0 m			
Solar irradiance (W/m^2)	Exp. $V_{ch.\ base}$ (m/s)	Num. $V_{ch.\ base}$ (m/s)	Error %	Solar irradiance (W/m^2)	Exp. $V_{ch.\ base}$ (m/s)	Num. $V_{ch.\ base}$ (m/s)	Error %
806	1.56	1.6	2.5	808	2.25	2.34	2.22

5 Conclusions

Experimental and numerical studies have been conducted on SC models with four different collector diameters. Results demonstrate that as the collector diameter increases, the system performance enhances. But, during the solar time, thermal efficiency of the collector is reduced as the collector diameter increased due to the high thermal losses to the environment.

The authors acknowledge Universiti Teknologi PETRONAS (UTP) in Malaysia for the logistic and technical support to produce this work. The first author appreciates the financial support from Iraqi government through sponsoring her PhD study under full scholarship.

References

1. E. Lorenzo, "De Los Archivos Históricos de la Energía Solar; Las chimeneas solares: De una propuesta española en 1903 a la Central de Manzanares,"(2002)
2. I. Cabanyes, Las chimeneas solares (Solar chimneys), La ernergia eléctrica, (1903)
3. M. A. dos Santos Bernardes. *Solar Energy,* A. Belmiloudi, Ed.: InTech, (2011)
4. C. Papageorgiou, Solar Energy, Ed.: R.D. Rugescu, 187-222 (2010)
5. N. Pasumarthi and S. Sherif, International Journal of Energy Research **22**, pp. 277-288, (1998)
6. J. Schlaich, R. Bergermann, W. Schiel, and G. Weinrebe, International: Journal of the International Association for Bridge and Structural Engineering (IABSE) **14**, pp. 225-229, (2004)
7. J. Schlaich, *The solar chimney: Electricity from the sun*: Edition Axel Menges, (1995)
8. J. Schlaich, R. Bergermann, W. Schiel, and G. Weinrebe, Journal of Solar Energy Engineering, Transactions of the ASME **127**, pp. 117-124, (2005).
9. M. A. d. S. Bernardes, MSc Theses published by Stuttgart: IER, Bibliothek, (2004) http://dx.doi.org/10.18419/opus-1630
10. D. Bonnelle. Doctoral thesis, University Claude Bernard-Lyon 1, France, 2004
11. J. P. Pretorius and D. G. Kröger, Solar Energy, **80**, 535-544, (2006)
12. E. Bilgen and J. Rheault, Solar Energy **79**, 449-458, (2005)
13. A. Koonsrisuk, S. Lorente, A. Bejan, Constructal solar chimney configuration, Int. J. Heat. Mass Transfer **53.** 327-333 (2010)
14. R. S. Vieira , A. P. Petry , L. A. O. Rocha , L.A. Isoldi and E. D. dos Santos. Renewable Energy **109.** 222-234 (2017)